ISBN: 978-3-95450-247-9 ISSN: 2673-5490 doi: 10.18429/JACoW-IPAC2024-THPC16

SORTING STRATEGIES FOR THE NEW SUPERCONDUCTING MAGNETS FOR THE CERN HL-LHC*

T. Pugnat, M. Giovannozzi, E. Todesco, R. Tomás, A. Wegscheider, CERN, Geneva, Switzerland

Abstract

In a circular collider, precise control of the linear optics in the vicinity of the interaction points plays a crucial role in ensuring optimal operational performance and satisfying the machine protection constraints. Superconducting magnets are affected by unavoidable field errors that impact machine performance, and mitigation strategies are usually put in place to improve the situation. Past studies performed on the LHC and HL-LHC have shown the benefit of magnet sorting on both initial beta-beating, through compensation of magnetic field errors, and overall correction quality of the machine optics. This work aims to extend the studies carried out in the context of HL-LHC by considering the possible impact on performance of various sorting strategies applied to the new triplet quadrupoles for the ATLAS and CMS high-luminosity insertions.

INTRODUCTION

In the context of the LHC high-luminosity upgrade (HL-LHC) [1], the main magnets of both high-luminosity insertion regions will be replaced. This includes the superconducting Inner Triplet quadrupoles (IT), which will be replaced by magnets with a larger aperture to reach a smaller β^* in the high-luminosity interaction points (IP) in the ATLAS and CMS experiments. With and all IT quadrupoles for a given side of each interaction point powered in series, the adjustment capabilities for the gradient of individual magnets are limited. Therefore, errors in the magnet transfer function (TF), which are unavoidable for superconducting magnets, need to be considered as a perturbation that should be mitigated, which can be achieved by performing sorting of the magnets, as discussed in this paper.

THE SORTING PROCEDURE

Optics and Magnet Transfer Function

The HL-LHC IT quadrupoles are Nb_3Sn magnets, and have an aperture of 150 mm [1] to be compared to the 70 mm for the LHC [2]. Their maximum operational gradient is 132.2 T/m at 7 TeV. Two families make up this group. The elements Q1 and Q3 are made of two magnets (A and B) in a single cryostat with a total magnetic length $L_m = 2 \times 4.2$ m) [1]. The Q2 is composed of a pair of magnets (A and B) in two different cryostats each with a magnetic length $L_m = 7.15$ m) [1, 3] (see Fig. 1). Each group of Q1, Q2A, Q2B and Q3 magnets is powered in series by means of an 18 kA power supply. Q1 and Q3 each have an additional ± 2 kA trim power supply that provides individual current adjustment [1]. This allows the average TF error of the magnets in a given circuit to be corrected, but not the deviations for individual magnets, but this is crucial, in particular for Q2 [4, 5]. In our studies, the deviation of the TF from its nominal value (corresponding to a deviation of the gradient $\Delta K_{1,i}/K_{1,i}$) is modelled using a Gaussian distribution cut at 3σ, with $3\sigma = 25 \times 10^{-4}$. This corresponds to the new criteria for the specification of IT magnets, without systematic effects or uncertainty on the measurement of the TF [6–8].

Previous studies [4, 5], focusing on the correctability of the optics with TF errors, concluded that the difference in TF error in each Q2 circuit should be less than 2×10^{-3}. Here, we focus on minimising the β-beating, which is generated by the TF errors of IT quadrupoles. The β-beating achievable after beam-based corrections of the optics will be considered in future studies. This analysis is performed considering squeezed round optics at nominal beam energy. The tunes were set to $Q_x = 62.31$ and $Q_y = 60.32$, the chromaticities at $Q'_x = Q'_y = 2$ and $\beta^* = 0.15$ m in the ATLAS and CMS insertions.

Pairing and Swapping

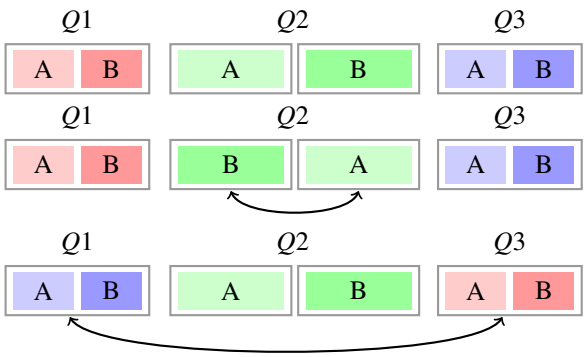

Figure 1: Pairing possibilities for one side of one IP are shown: Initial configuration (top); pairing of two Q_2 assemblies (centre); swapping of Q1 and Q3 (bottom).

A Python script was developed to sort the magnets and find the configuration with minimum β-beating by checking all the magnet combinations using a score function. Hardware features exclude some combinations. For example, Q1 and Q3 cannot be exchanged with Q2. The generation of possible magnet arrangements should consider the options illustrated in Fig. 1:

Pairing: Triplet magnets of the same family can be swapped, e.g. between A and B for Q2, and between Q1 and Q3, remaining in the same IP side.

Swapping: Magnets of the same family can be exchanged between IPs and IP sides.

* RESEARCH SUPPORTED BY THE HL-LHC PROJECT.

ISBN: 978-3-95450-247-9 ISSN: 2673-5490 doi: 10.18429/JACoW-IPAC2024-THPC16

Hardware Constraints

Despite considerable efforts made to standardise the cryo-assemblies during the design stage, cryogenic requirements and the tunnel layout impose a certain number of variations in hardware configurations. These differences are implemented at different stages of assembly. Therefore, an early decision on the tunnel location of a given cryo-assembly benefits from a larger number of locations being compatible with the hardware, which maximises the degrees of freedom for sorting. The following phases have been identified in the preparation process of a cryo-assembly:

- **Phase 1**: assembly of the main part of the cryostat, main vacuum vessel, thermal shield, cold mass supports and instrumentation feedthroughs.
- **Phase 2**: after the powering tests, equipment specific to the installation slot is added.
- **Phase 3**: installation of beam vacuum equipment.

Table 1: Number of Combinations for Each Phase of the Cryo-assembly Preparation

Phase	Description	Number
1	8 possibilities for Q1/Q3	8! = 40320
	8 possibilities for Q2A/B	8! = 40320
2	8 possibilities for Q1/Q3	8! = 40320
	4 possibilities for Q2A	4! = 24
	4 possibilities for Q2B	4! = 24
3	2 possibilities for Q1	2! = 2
	2 possibilities for Q3	2! = 2
	2 possibilities for Q2	2! = 2

The resulting number of combinations after each phase is listed in Table 1. It was not possible to test all 1'625'702'400 combinations, as it takes several weeks to perform a complete simulation for a single sequence of TF errors.

It was decided to proceed in two steps with the sorting procedure of a sequence of 24 TF errors for the IT magnets. A "1st sorting" is performed considering the 8! cases of reordering of each of the magnet families (Q1/Q3 and Q2 separately) and the minimum β-beating is retained. Note that when a magnet family is considered, the TF errors of the others are set to zero. Then, a "2nd sorting" merges together the 100 reordered sequences providing the lowest β-beating for each of the two families, and the β-beating is re-evaluated, which allows probing the compensations of TF errors between the two magnet families.

Scoring Function

The first step of the study was to determine the correlation between the various observables at hand. Using the Pearson coefficient r, a lower correlation between horizontal and vertical β-beating is observed compared to that between RMS and maximum β-beating in the same plane (see Fig. 2). It is also visible that Q2s have a stronger impact on the β-beating than Q1/Q3, due to the higher values of the β-functions in the Q2s. The chosen score function is:

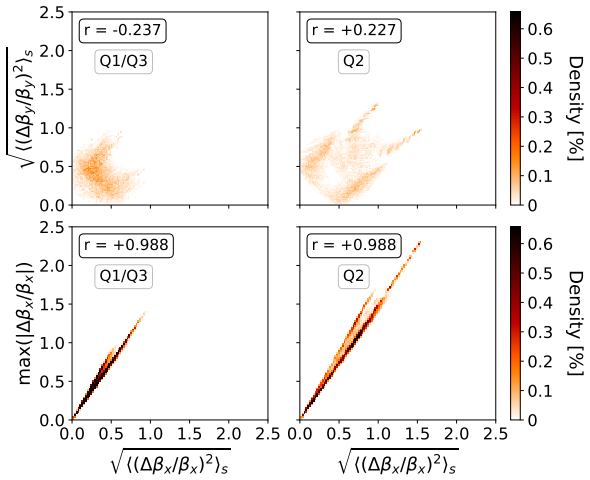

Figure 2: 2D histogram of the RMS vertical β-beating (top) and maximum horizontal β-beating (bottom) as a function of the RMS horizontal β-beating for all permutations of Q1/Q3 (left) and Q2 (right).

$$\text{score} = \sqrt{\left\langle\left(\frac{\Delta\beta_x}{\beta_x}\right)^2\right\rangle_s + \left\langle\left(\frac{\Delta\beta_y}{\beta_y}\right)^2\right\rangle_s}, \qquad (1)$$

where $\langle\ \rangle_s$ indicates the average over all arc BPMs. Note that a score of, e.g. 0.2 corresponds to a RMS horizontal beta-beating of ≈ 0.18.

To speed up the computation of the β-beating, the standard analytical formula based on the nominal optics has been implemented, namely:

$$\frac{\Delta\beta_z}{\beta_z}(s) = \mp\sum_i \Delta K_{1,i}\beta_{z,i}\frac{\cos\left(4|\psi_{z,i}(s)| - 2\pi Q_z\right)}{2\sin(2\pi Q_z)}, \qquad (2)$$

with $z = x, y$, $\Delta K_{1,i}$ the ith integrated TF error, and $\psi_{z,i}(s)$ the phase advance between the ith magnet and the position s. This is a first-order approximation in $\Delta K_{1,i}$, and these errors might prevent one from finding stable optics. Figure 3 shows this effect using colours to label error configurations that generate stable (green) or unstable (red) optics. A clear threshold can be observed when either of the mean β-beatings is greater than 0.1 – 0.2. For RMS and absolute maximum β-beating, no clear separation can be observed, but unstable optics appears gradually when the observables are higher than 0.5 and 0.75, horizontal and vertical, respectively.

RESULTS

The numerical simulations consist of 1000 sequences of TF errors. For each sequence, the β-beating is estimated for the initial ordering, using the best permutations after the "1st sorting" and after the "2nd sorting".Figure 4 shows the distribution of the horizontal and vertical RMS β-beating and the score function after each step. MAD-X provides very similar results, although the optics for the initial error distribution is unstable in 41 % of the cases.

ISBN: 978-3-95450-247-9 ISSN: 2673-5490 doi: 10.18429/JACoW-IPAC2024-THPC16

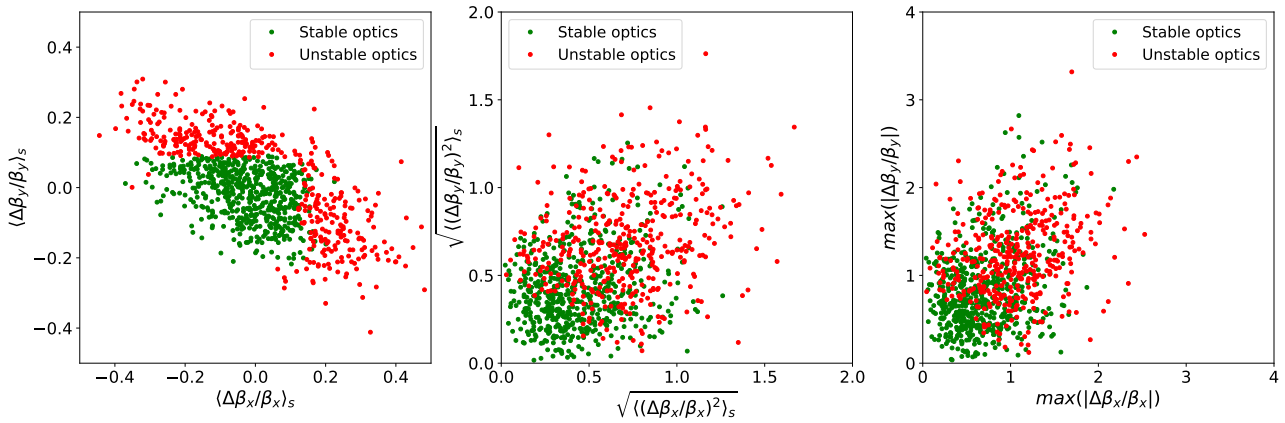

Figure 3: Correlation plots for some β-beating-related observables (from Eq. (2)) in the horizontal and vertical plane, calculated using 1000 permutations of an initial set of errors in the IT TFs. The colours indicate the optics stability.

A clear improvement in β-beating is already observed with 1st sorting, and the second step further reduces it. The β-beating for the initial distribution of errors can be as high as 1.5 (but could reach even higher values, up to 3.3, considering combinations of the worst 100 permutations of both families). The extreme values of the distributions move from approximately 1.5 to 0.6 and 0.5 in the horizontal and vertical planes, respectively. Although the improvement in 2nd sorting appears to be small compared to 1st sorting.

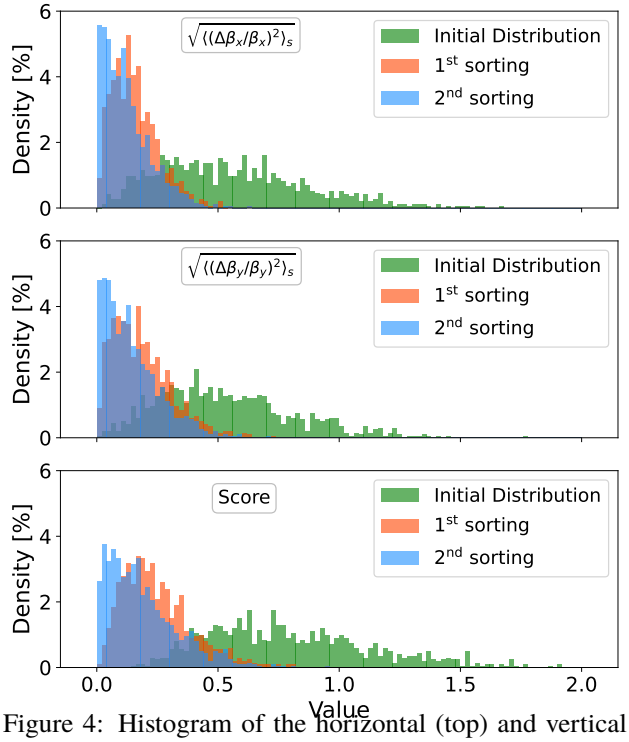

Figure 4: Histogram of the horizontal (top) and vertical (middle) RMS β-beating, and score function (bottom) for the three stages of magnets reordering.

Figure 5 shows the correlation between the initial situation and the results after sorting for the case of vertical RMS β-beating (top) or the score function (bottom). In total, most configurations are below the straight line $y = x$, indicating that it is possible to improve the initial configuration.

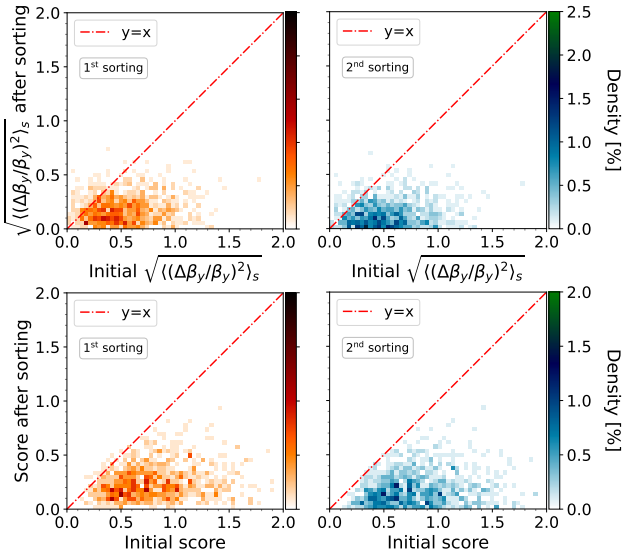

Figure 5: Distribution of the correlation for the vertical RMS β-beating (top) and score (bottom) due to the 1st sorting (left) and 2nd sorting (right).

CONCLUSIONS AND OUTLOOK

The application of a sorting procedure to cope with TF errors of IT triplet quadrupoles of the HL-LHC has been shown to significantly improve the resulting β-beating. The fraction of sequences for which the score function is below 0.2 after sorting reaches approximately 62 %, while without sorting this fraction is approximately 0.5 %. More analysis and optimisations are still needed, as the efficiency of beam-based optics corrections still needs to be determined, and recent measurement results indicate that the spread of TF errors will be smaller than the currently assumed value. Other possibilities of finding the global minimum of the β-beating without testing the totality of configurations of the two families of magnets will also be explored.

ISBN: 978-3-95450-247-9 ISSN: 2673-5490 doi: 10.18429/JACoW-IPAC2024-THPC16

REFERENCES

[1] O. Aberle *et al.*, *High-Luminosity Large Hadron Collider (HL-LHC): Technical design report*. CERN, 2020, doi:10.23731/CYRM-2020-0010

[2] O. S. Brüning *et al.*, *LHC Design Report*. CERN, 2004, doi:10.5170/CERN-2004-003-V-1

[3] S. Izquierdo Bermudez, *MQXFS test results*, 2023, https://indico.cern.ch/event/1293138/contributions/5474429/attachments/2722450/4731405/2023_09_vancouver_mqxfs_test_results.pdf

[4] X. Buffat *et al.*, "Optics Measurement and Correction Strategies for HL-LHC," CERN, Tech. Rep., 2022, https://cds.cern.ch/record/2808650

[5] R. Tomas Garcia, *Preview of the procedures for linear and nonlinear optics correction and assumptions underlying*, 2019, https://indico.cern.ch/event/806637/contributions/3573636/attachments/1926732/3189951/SLIDESlogo.pdf

[6] A. B. Yahia, *Production testing summary of the MQXFA magnets*, 2023, https://indico.cern.ch/event/1293138/contributions/5474420/attachments/2722417/4730101/MQXFA_Vertical_Test_HiLumi_CM_2023_v2.pdf

[7] J. DiMarco, *LQXFA/B01 magnetic measurements*, 2023, https://indico.cern.ch/event/1293138/contributions/5474434/attachments/2723160/4731616/LQXFA01_magMeas_collabMeeting_27Sep2023.pdf

[8] L. Fiscarelli, *Field quality and integrated gradient in MQXFB*, 2023, https://indico.cern.ch/event/1293138/contributions/5474435/attachments/2722490/4731613/LFiscarelli_MM_on_MQXFB_20230924_c.pdf